Mapping Agricultural Crops with AVIRIS Spectra in Washington State

Robert O. Green, Betina Pavri, Dar Roberts, and Susan Ustin

Jet Propulsion Laboratory, California Institute of Technology
Pasadena, CA 91109

1.0 Introduction

Spectroscopy is used in the laboratory to measure the molecular components and concentrations of plant constituents to answer questions about the plant type, status, and health. Imaging spectrometers measure the upwelling spectral radiance above the Earth's surface as images. Ideally, imaging spectrometer data sets should be used to understand plant type, plant status, and health of plants in an agricultural setting. An Airborne Visible/Infrared Imaging Spectrometer (AVIRIS) data set was acquired over agricultural fields near Wallula, Washington on July 23rd, 1997 (Figure 1). AVIRIS measures upwelling radiance spectra through 224 spectral channels with contiguous 10-nm sampling from 400 to 2500 nm in the solar-reflected spectrum. The spectra are measured as images of 11 by up to 800 km with 20-m spatial resolution. The spectral images measured by AVIRIS represent the integrated signal resulting from: the solar irradiance; two way trasmittance and scattering of the atmosphere; the absorptions and scattering of surface materials; as well as the spectral, radiometric and spatial response functions of AVIRIS. This paper presents initial research to derive properties of the agricultural fields near Wallula from the calibrated spectral images measured by AVIRIS near the top of the atmosphere.

2.0 Data and Atmospheric Correction

AVIRIS data are delivered as the calibrated spectral radiance measured at the sensor. Radiance spectra from five of the fields in the Wallula AVIRIS data set show differences, but are dominated by the solar source function and the absorption and scattering of the atmosphere (Figure 2). A radiance to reflectance inversion algorithm (Green et al. 1993) based in part on the MODTRAN radiative transfer code (Berk et al. 1989, Anderson et al. 1995) was used to derive the apparent surface reflectance of the Wallula data set. The algorithm compensates for atmospheric water vapor, Rayleigh scattering, aerosol scattering, as well as the absorption of well mixed gases and ozone. The surface reflectance is calculated based on the observational geometry of the AVIRIS sensor and the position of the sun. A horizontal surface appropriate for agricultural fields is assumed. Surface reflectance spectra for the five fields of the Wallula data set (Figure 3) show the the solar and atmospheric effects in the measured radiance spectra are compensated by this algorithm. Surface reflectance was not derived for narrow regions of the spectrum near 1400 nm and 1900 nm absorption due to the strong absorption by atmospheric water vapor. In the derived reflectance spectra, the absorption and scattering signatures of the important molecules and constituents of plants in the agricultural fields are expressed. At the reflectance level, the spectrum from each field is different from the others. This difference in reflectance provides the basis for deriving information about the different crops.

3.0 Analysis and Results

To isolate the different spectral characteristics of the agricultural fields, spectral fitting was used to derive the apparent abundance of different molecular constituents expressed in the spectrum. The first molecular constituent derived was the expressed liquid water absorption based on the 980-nm spectral feature. A spectral fitting algorithm was applied to assess the strength of the liquid-water absorption. A wide variation in expressed liquid water in plants is shown across the agricultural fields of the Wallula AVIRIS data set (Figure 4). Close examination of the liquid water image reveals fields that were being actively irrigated at the time of the AVIRIS acquisition. Bright, high liquid water, radii appear in the crop circle with active irrigation caused by the liquid water drops

on the vegetation. A second spectral fit for liquid water was calculated based on the liquid water absorption expressed at 1180 nm in the spectrum. The light scattering of vegetation is reduced at 1180 nm relative to 940 nm; consequently, the expressed liquid water is dominated more by the top of the vegetation canopy. The 1180-nm liquid water image also shows a wide variation in the expressed liquid water abundance across the Wallula AVIRIS data set (Figure 5). The variation in expressed liquid water absorption within and between the two spectral regions provides information both about plant leaf water and the plant canopy scattering characteristic.

The most important molecule in plants is chlorophyll. A spectral fitting alogorithm was applied to the Wallula data set to assess the strength of the chlorophyll absorption in the 450- to 700-nm region of the spectrum. The expressed strength of the chlorophyll absorption varies over a wide range of values across the spectral image (Figure 6). The derived chlorophyll and the liquid-water absorption do not correlate strongly. This lack of correlation is due to actual differences in the chlorophyll and liquid-water content of the vegetation. In addition, the lack of correlation results from the enhanced expression of liquid water due to multiple scattering in the canopy at 980 nm and 1180 nm. The strong absorption of chlorophyll precludes significant multiple scattering. The liquid-water and chlorophyll images provide different, but complementary, information about the characteristics of the plants in the agricultural fields at Wallula, Washington.

The final molecular absorption assessed in the AVIRIS agricultural images was cellulose. Cellulose shows strong absorption features in the 2100-nm and 2300-nm regions of the spectrum. A spectral-fitting algorithm was applied to assess the combined strength of these absorptions across the Wallula data set (Figure 7). A range of cellulose values results from the spectral fitting analysis. The cellulose image is more noisy than that for liquid water or for chlorophyll. This increased noise results from the strong overprint of the liquid-water absorption on the cellulose absorption in the 2000-nm to 2500-nm spectral region. However, in the fields with uniform derived cellulose, the cellulose information contributes to characterization of the agricultural vegetation.

The expressed abundances of the different molecular constituents derived through spectral fitting were used to group the agricultural fields into similar crop types. A field visit after the AVIRIS data acquisition and after initial analysis of the data was used to attach labels to the different spectra and expressed molecular abundances (Figure 8). Identification of agricultural crop type is a required first step before extracting useful plant status and plant health information for the AVIRIS spectral images.

4.0 Summary

AVIRIS spectral images were acquired over a group of agricultural fields in the Wallula Washington area on the 23rd of July 1997. The calibrated AVIRIS radiance spectra were inverted from total upwelling spectral radiance to surface reflectance. In surface reflectance the inherent molecular absorptions and scattering characteristics of the agricultural plants are expressed. A spectral fitting algorithm was applied to the AVIRIS reflectance spectra to assess the expressed abundance of the molecules liquid water, chlorophyll, and cellulose in the agricultural vegetation. Wide variations in the expressed molecular absoprtions were found across the AVIRIS Walulla data set. For liquid water, two different portions of the spectrum were assessed with the spectral fitting algorithm. The expressed liquid water differed between the 980-nm and 1180-nm derivation. This is expected based on the differential penetration of the radiance into the plant canopy. The expressed chlorophyll absorption varied widely across the data set. Chlorophyll and liquid water absorption were found not to be strongly correlated. This is explained by the high level of multiple scattering at 980 nm compared to the chlorophyll-dominated portion of the spectrum. Finally, cellulose was assessed based on the absorptions at 2100 nm and 2300 nm. As with water and chlorophyll, variation in the expressed cellulose abundance was found across the image. The AVIRIS surface reflectance spectra and derived molecular abundance were used to

group the agricultural field in the Wallula data set. A field visit was used to establish and verify the plant type in several of the fields. Future work will focus on moving beyond identification of plant type and towards assessment of plant status and health.

5.0 References

Anderson, G.P., J. Wang, and J.H. Chetwynd (1995), "MODTRAN3: An Update And Recent Validations Against Airborne High Resolution Interferometer Measurements," Summaries of the Fifth Annual JPL Airborne Earth Science Workshop, JPL Publication 95-1, Vol. 1: AVIRIS Workshop, R.O. Green, Ed., Jet Propulsion Laboratory, Pasadena, CA, 5-8.

Berk, A., L.S. Bernstein, and D.C. Robertson (1989), MODTRAN: A Moderate Resolution Model for LOWTRAN 7, Final Report, GL-TR-0122, AFGL, Hanscom AFB, MA, 42 pp.

Green, R.O., Conel, J.E., Roberts, D.A. (1993), Estimation of aerosol optical depth and additional amospheric parameters for the calculation of the reflectance from radience measured by the Airborne Visible/Infrared Imaging Spectrometer, Summaries of the Fourth Annual JPL Airborne Geoscience Workshop., JPL Publication 93-26, Vol. 1, AVIRIS Workshop, R.O. Green, Ed, Jet Propulsion Laboratory, Pasadena, CA, 73-76.

6.0 ACKNOWLEDGEMENTS

Figure 1. AVIRIS image of agricultural fields near Wallula, WA acquired on 23 July 1997.
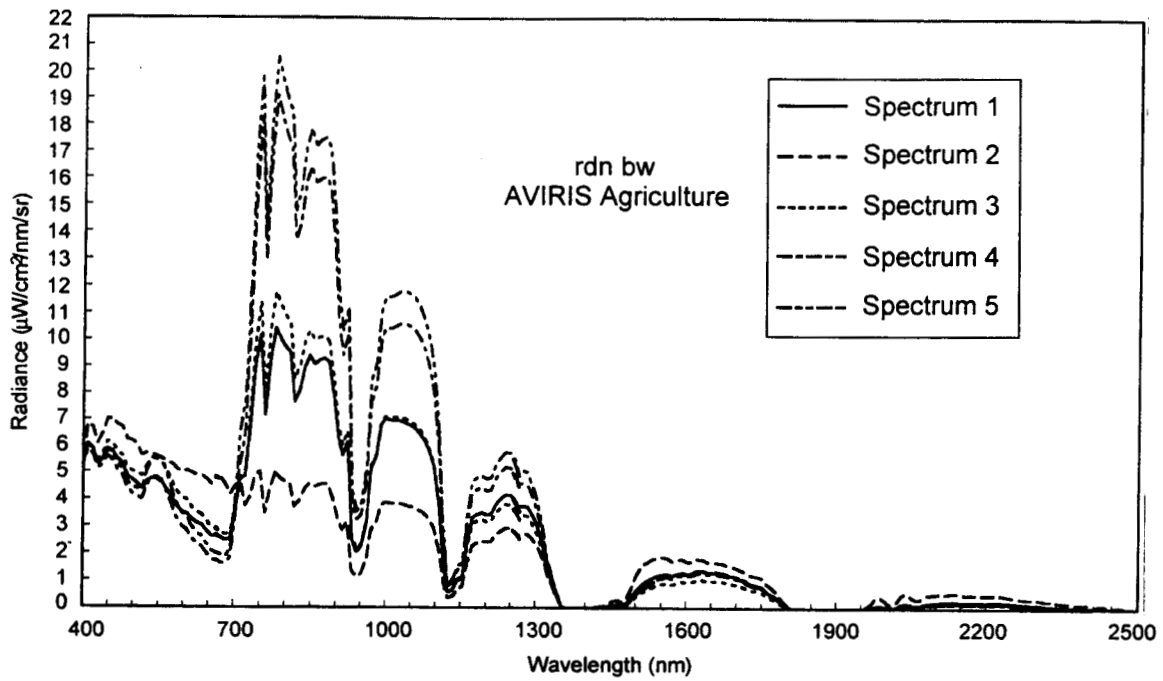
Figure 2.   AVIRIS calibrated radiance spectra of agricultural fields and background areas.
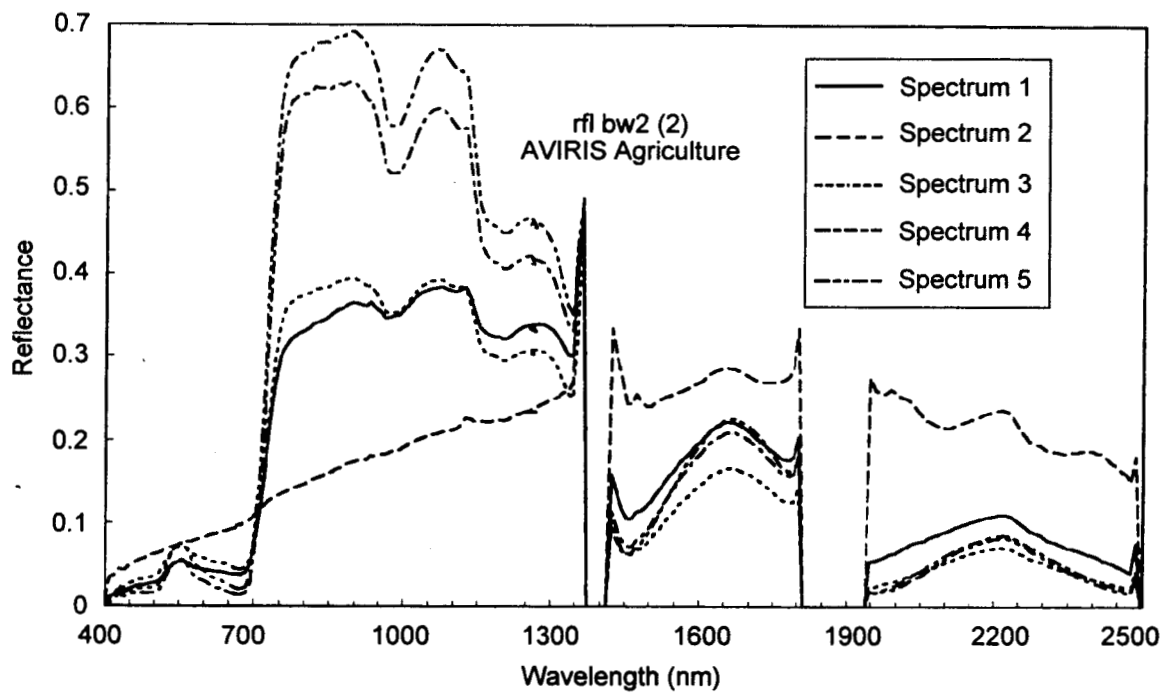

Figure 3. Derived surface reflectance spectra following radiance to reflectance inversion.
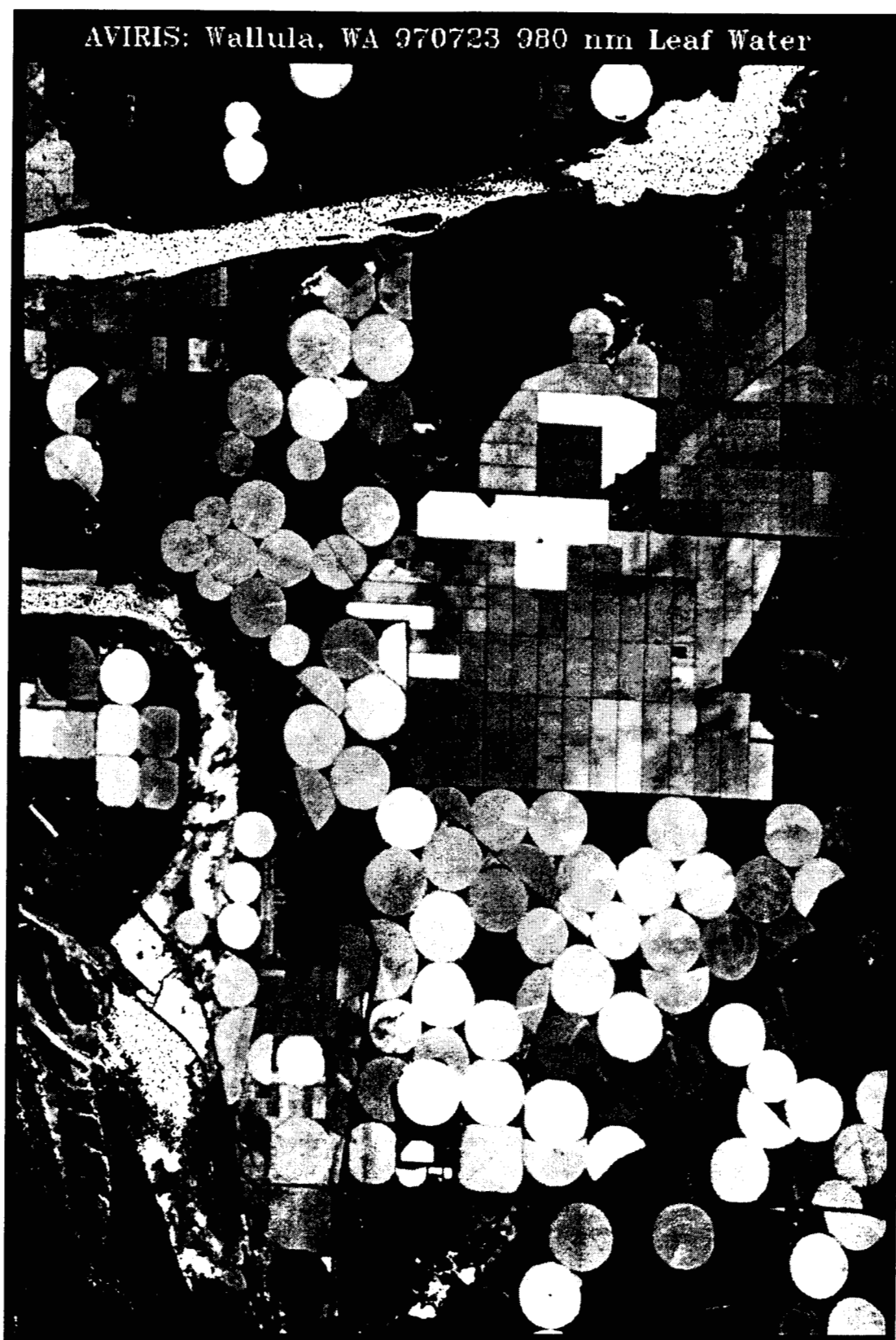
Figure 4. Spectral-fit 980-nm liquid-water image in equivalent transmittance microns. **High liquid water** is encoded as high image signal.
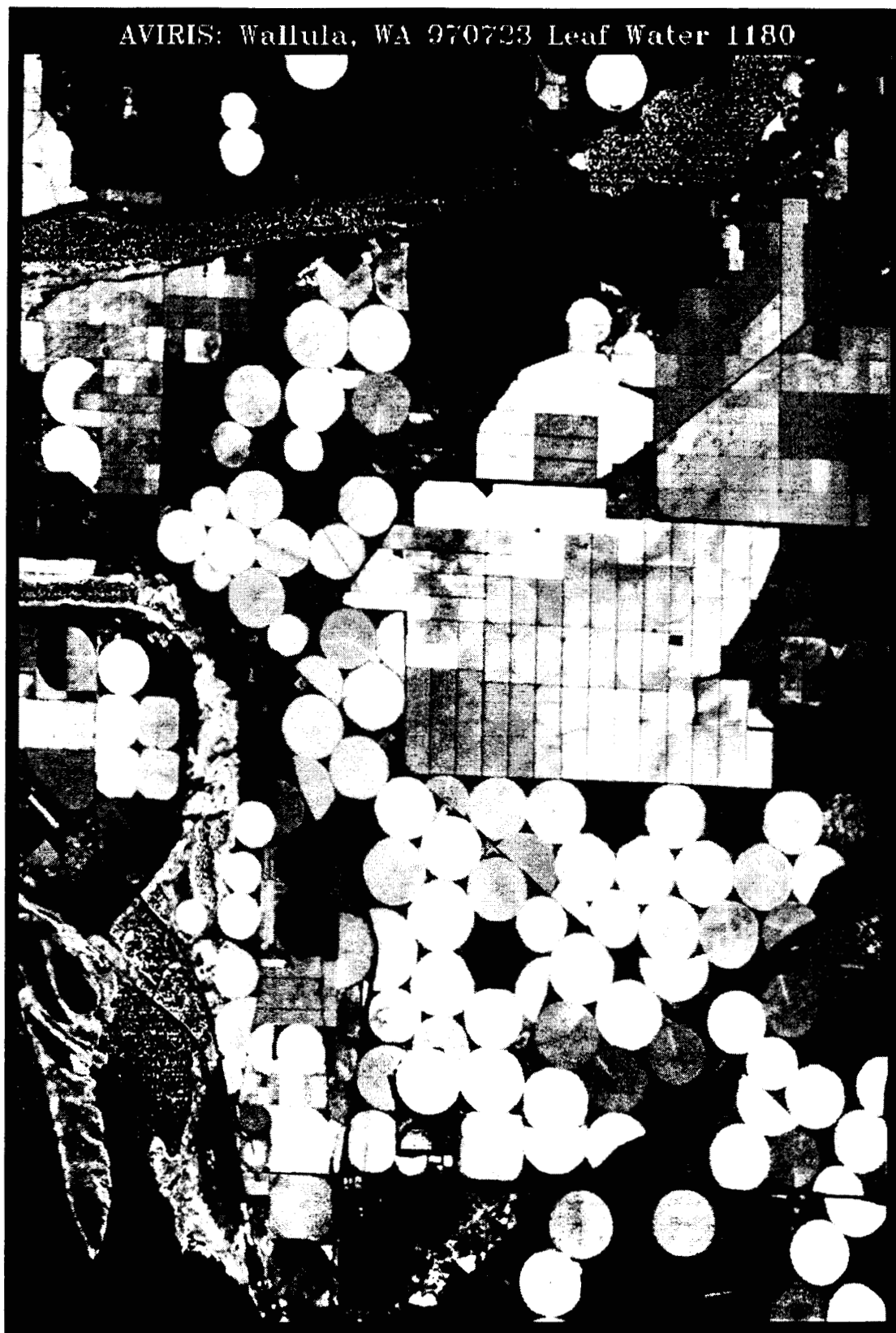
Figure 5. Spectral-fit 1180-nm liquid-water image in equivalent transmittance microns.
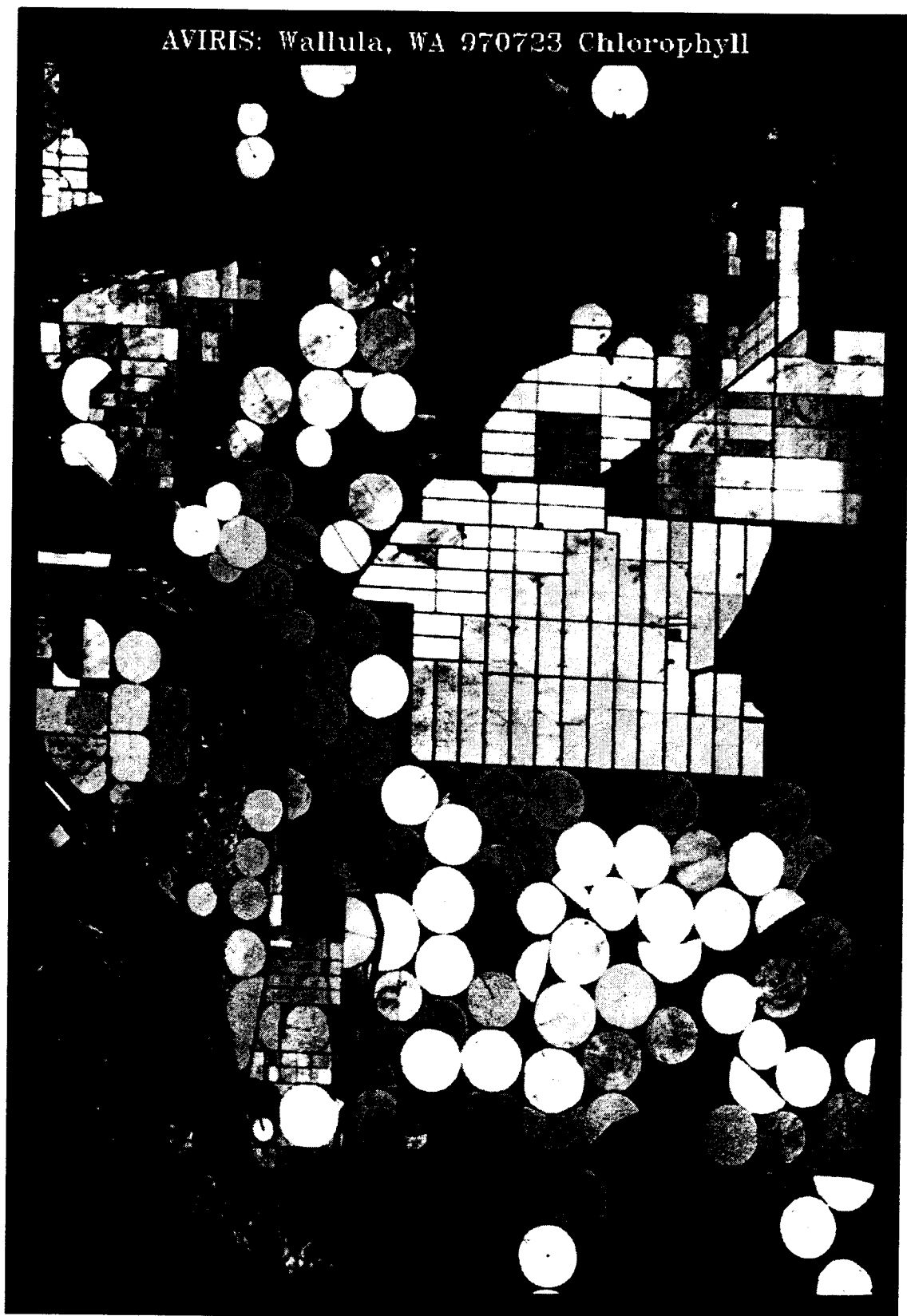
Figure 6. Spectral-fit chlorophyll image. High-chlorophyll absorption is encoded as bright **image** intensity.

Figure 7. Spectral-fit cellulose image. High-cellolose absorption is encoded as bright image intensity.
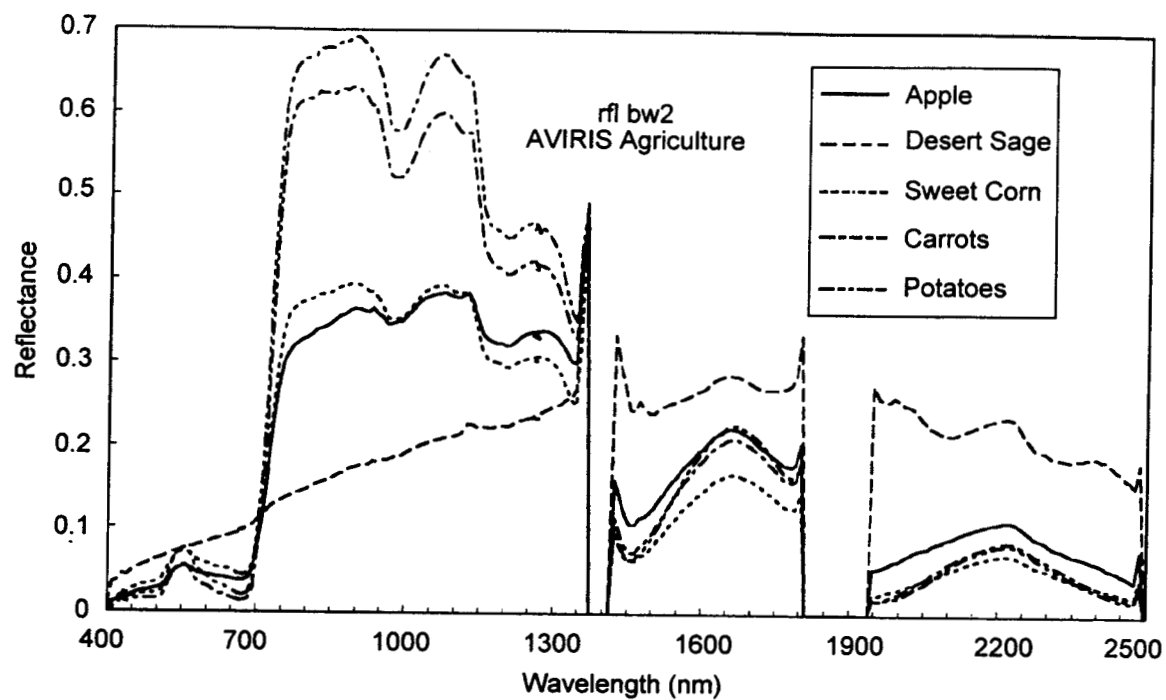
Figure 8. AVIRIS surface reflectance spectra of determined agricultural crops and background.